

## Ethyl 4-(4'-heptanoyloxyphenyl)-6-methyl-3,4-dihydropyrimidin-2-one-5-carboxylate Prevents Progression of Monocrotaline-induced Pulmonary Arterial Hypertension in Rats

S.M. Malik<sup>#</sup>, Satyanarayan Deep<sup>@</sup>, Rahul Ranjan<sup>#</sup>, A.K. Prasad<sup>@</sup>,  
D.N. Prasad<sup>#</sup>, S.B. Singh<sup>!</sup>, and Ekta Kohli<sup>#,\*</sup>

<sup>#</sup>DRDO-Defence Institute of Physiology and Allied Science, Delhi - 110 054, India

<sup>@</sup>Department of Chemistry, University of Delhi, Delhi - 110 007, India

<sup>!</sup>DRDO-Directorate of Life Sciences, New Delhi - 110 011, India

<sup>\*</sup>E-mail: [ektakohli@hotmail.com](mailto:ektakohli@hotmail.com)

### ABSTRACT

Therapies to prevent onset and progression of pulmonary arterial pressure are not very effective yet. This study was designed to investigate the effects of a novel dihydropyrimidinone, ethyl 4-(4'-heptanoyloxyphenyl)-6-methyl-3,4-dihydropyrimidin-2-one-5-carboxylate (H-DHPM) on pathogenesis of monocrotaline (MCT)-induced pulmonary arterial hypertension (PAH). For the same purpose, rats were injected intraperitoneally (i.p.) a single dose (60 mg/kg) of MCT which led to development of PAH in 21 days. MCT insult caused high mortality, pulmonary vascular and parenchymal remodelling. Since the course of PAH pathogenesis is characterised by an early onset and progression phases, H-DHPM was administered i.p. at 30 mg/kg dosage in MCT pre-injected animals either from day 0 through day 21 or day 14 through day 21 of MCT injection in two separate treatment groups. H-DHPM significantly improved survival, prevented remodelling of pulmonary vasculature and parenchyma and subsequently ameliorated PAH pathogenesis. Moreover, we observed significant decrease in right ventricle hypertrophy, measured by wet weight of right ventricle (RV) divided by wet weight of left ventricle plus septum (LV+S), in H-DHPM treated groups as compared to MCT injected animals. These findings suggest H-DHPM not only prevented development of PAH but also treated the PAH pathogenesis in progressive phase. In conclusion, our data determines H-DHPM, might be a future drug for the prevention of PAH.

**Keywords:** Monocrotaline; Pulmonary arterial hypertension; Calcium channel blockers; Right ventricle hypertrophy; Medial wall thickness; Apoptosis; Nitric oxide; H-DHPM

### NOMENCLATURE

PH	Pulmonary hypertension
RVH	Right ventricle hypertrophy
RVSP	Right ventricle systolic pressure
MCT	Monocrotaline
H-DHPM	ethyl 4-(4'-heptanoyloxyphenyl)-6-methyl-3,4-dihydropyrimidin-2-one-5-carboxylate
CCB	Calcium channel blockers
PVR	Pulmonary vascular resistance

### 1. INTRODUCTION

Pulmonary arterial hypertension (PAH), defined by a rise in mean pulmonary arterial pressure above 25 mmHg at rest, is a progressive disease characterised by pulmonary vasoconstriction and gradual precapillary arterial remodelling leading to pulmonary vascular resistance (PVR)<sup>1</sup>. Impedance in circulation by PVR leads to right ventricular remodelling, frequently terminating into right heart failure and premature mortality<sup>2,3</sup>. Vascular remodelling befalls predominantly due to pulmonary artery smooth muscle cell (PASMC) proliferation, migration and pulmonary artery endothelial cells (P-EC)

dysfunction<sup>4,5</sup>. Various therapeutic strategies like vasodilators, diuretic therapy, inhaled nitric oxide therapy, intravenous prostacyclin, phosphodiesterase inhibitors, endothelin antagonists and anticoagulant agents have been employed to manage PAH.<sup>2</sup> However, due to limited effectiveness, high cost and serious side effects, an appropriate therapy is still lacking. To achieve the goal of finding better therapeutic targets, the course of disease needs to be followed in order to evaluate the changes in early and progressive phases of PAH pathogenesis.

Monocrotaline (MCT), a pyrrolizidine alkaloid from *Crotalaria* plant, is bioactivated in liver to monocrotaline pyrrole (MCTP), which is a potent pneumotoxin<sup>6</sup>. Numerous researchers have established that a single dose of MCT (intraperitoneal or subcutaneous) induces PAH in animals by pulmonary endothelial damage, medial hypertrophy of the pulmonary arteries, and subsequently right ventricular remodelling<sup>6</sup>. Recent evidences suggest MCT induces endothelial dysfunction and consequent pulmonary arterial hypertension, by binding to extra cellular calcium sensing receptor (CaSR)<sup>7</sup>. Calcium (Ca<sup>2+</sup>) channel pathway has been previously related to play a key role in vasoconstriction and remodelling of pulmonary vessels. Intracellular Ca<sup>2+</sup>[Ca<sup>2+</sup>]<sub>i</sub> acts

as a secondary messenger and its imbalance can greatly influence pathophysiology of PAH by inducing PSMC proliferation and P-EC instability<sup>7</sup>. Calcium channel blockers (CCBs), which are a class of drugs that avert entry of Ca<sup>2+</sup> into cardio myocytes, PSMC and P-EC, hence preclude contractility of heart and constriction of pulmonary arteries (PA)<sup>8-11</sup>. Previously, long acting CCBs (dihydropyrimidine) like nifedipine, diltiazem, nicardipine, felodipine and amlodipine have been used in ameliorating effects of increased Ca<sup>2+</sup> insurgency into cytosol to treat pulmonary arterial remodelling<sup>9,12-16</sup>.

Dihydropyrimidinone (DHPM), a derivative of dihydropyrimidine and class of CCBs have antihypertensive effects; however, no established data is available on its use in treating PAH<sup>17</sup>. Of note, the structural modifications greatly influence function of pyrimidinones and recently, Munral<sup>16,18</sup>, *et al.* synthesised a novel CCB, a modified DHPM, namely ethyl 4-(4'-heptanoyloxyphenyl)-6-methyl-3,4-dihydropyrimidin-2-one-5-carboxylate (H-DHPM). H-DHPM, a versatile CCB, has been reported to have better functional efficacy as compared to parent moiety OH-DHPM<sup>16,18</sup>. The activity of H-DHPM in blocking Ca<sup>2+</sup> activity has been attributed by the authors to an acyl (heptonyl) group at C-4' position of the compound. Priya<sup>18</sup>, *et al.* have reported H-DHPM as an effective CCB with antithrombotic activity. It has been further suggested in the study that H-DHPM has highest Ca<sup>2+</sup> channel blocking capability as compared to other CCBs. Given the above mentioned rationale, in the present study, we investigated the beneficial effects of H-DHPM on MCT-induced PAH.

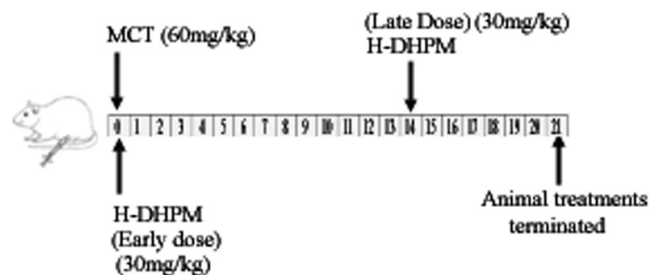
## 2. METHODS

### 2.1 Animal Model and Experimental Design

All experiments were carried out on male adult Sprague-Dawley rats (200 g to 250 g). The rats were housed in the experimental animal facility of the institute and on standard diet with deionised water (*ad-libitum*). All animal procedures were conducted in accordance with Committee for Purpose of Control and Supervision of Experimental Animals (CPCSEA), Government of India.

In the current study, 15 animals were assigned to each group. Animals were categorised into groups as shown in Table 1. The rationale for the decision of choosing the dosage was based upon publication of Priya<sup>18</sup>, *et al.*, wherein they had used the drug at 52 mg/kg p.o. Drug (H-DHPM) was dissolved in DMSO (50 %v/v). H-DHPM was administered to rats either from day 0 of MCT injection or from 14 day of MCT injection as explained in Table 1.

### Study protocol



### 2.2 Chemicals and Reagents

All Chemicals and reagents were purchased from Sigma-Aldrich (USA). Masson's trichrome Stain (HT15-1KT) was purchased from Sigma Aldrich (USA). ApoptTag Red In Situ Apoptosis Detection Kit (S7165) was purchased from Millipore (USA).

### 2.3 Synthesis of H-DHPM

H-DHPM was synthesised as described previously at Department of Chemistry, University of Delhi, Delhi, India. The physical and chemical characteristics of the H-DHMP have been previously explained and were reproduced for present study<sup>16,18</sup>.

### 2.4. Hemodynamic Measurements

After anesthetizing rats with 1.2 mg/kg (i.p.) urethane, rats were rested in supine position followed by making an incising on skin from mandible to sternum to expose the right jugular vein followed by bluntly nicking the vein. Right ventricular systolic pressure (RVSP) was measured by inserting a micro-tip catheter (3.0 F, Millar Instruments, Houston, USA) and passing it through jugular vein to right ventricle. RVSP was recorded and analysed by the Power Lab Data Acquisition system using Lab Chart 7 software (AD Instruments, Australia). The obtained results were plotted using Prism5 (GraphPad San Diego, CA, USA) for statistical analysis. After hemodynamic measurements were obtained, rats were euthanised with overdose of urethane (3 gms/kg; i.p.)

### 2.5 Histology and Morphometry

After euthanizing, the rats were perfused with PBS followed by 4 per cent PFA. Heart and lungs were harvested *en-bloc*, hearts was separated from lungs. The right ventricle

Table 1. Animal grouping and dosing

Group	Designation	Dosage; Route	Day of dosage	Regime of dosage
Control	C	N/A	Nil	N/A
Monocrotaline injected	MCT	60 mg/kg; i.p.	1 day	Single dose
Monocrotaline injected and H-DHPM early dose	MCT+ED	MCT: 60 mg/kg, H-DHPM: 30 mg/kg; i.p.	MCT: 1day, H-DHPM: daily for 21 days	12 h after MCT dose H-DHPM was given i.p. H-DHPM was administered daily for 21 days
Monocrotaline injected and H-DHPM late dose	MCT+LD	MCT: 60 mg/kg, H-DHPM: 30 mg/kg; i.p.	MCT: 1day, H-DHPM: daily for 7 days	14 days after MCT dose H-DHPM was given i.p. H-DHPM was administered daily for 7 days
Dimethyl Sulphoxide injected	DMSO	Proportional to treatment volume	21 days	Daily

(RV) was separated from the left ventricle (LV) plus ventricular septum and the wet weights were recorded. RV hypertrophy, determined by Fulton's Index (FI), was expressed as the ratio of RV to LV plus ventricular septum ( $FI=RV/LV+S$ ). Separately, lungs were instilled with 10 per cent formalin by tracheal installation and ligated with silk suture and left overnight. Left lung was dissected out and distal zone of left lung was prepared for paraffin embedding. 5  $\mu$ m thick sections of paraffin-embedded lung tissue were deparaffinised using xylene, followed by treatment with gradient ethanol and then washing with PBS. For histological analysis, tissues were stained with haematoxylin and eosin (H&E). For morphometry of distal pulmonary arteries, the medial wall thickness were measured in approximately 40 distal pulmonary arteries (between 25-200 $\mu$ m) per animal. The average was calculated using the formula<sup>19</sup>.

For Masson's trichrome staining (MTS), Trichrome Stain (Masson) Kit (cat no. HT15, Sigma Aldrich) was used as per manufactures protocol and 40 images per group were captured and analysed. Olympus BX 51 (Olympus) microscope was used for imaging at magnification of 40 x, and quantification of expression (using pixel intensity) was performed with ImageJ software from the National Institutes of Health and statistically evaluated by GraphPad Prism5.

## 2.6 TUNEL Assay

Apoptosis in lung tissue was detected by deoxynucleotidyl transferase dUTP nick end labeling (TUNEL) staining. ApopTag Red In-Situ Apoptosis Detection Kit was used to detect apoptotic cells in lung tissues according to the manufacturer's protocol. Briefly, 5 $\mu$ m thick sections of paraffin-embedded lung tissue were deparaffinised using xylene, followed by treatment with gradient ethanol and then washing with PBS. As a positive control (PC) of apoptotic cells, tissues were incubated in DNase I (0.5  $\mu$ g/ml) for 10 min at room temperature. Slides were counterstained for 5 min in DAPI (4',6-diamidino-2-phenylindole; a nuclear dye) and mounted. 10 views (images) per section at 40 x magnification were captured using Olympus BX51 (Olympus) microscope and analysed using ImageJ and statistically evaluated using Prism5 (GraphPad). Total number of TUNEL<sup>+</sup> was single blind analysed to avoid any bias. TUNEL<sup>+</sup>positive nuclei relative to total DAPI stained nuclei were counted using ImageJ(NIH) software.

## 2.7 Statistical Analysis

All data reported as mean  $\pm$  SEM. Statistical analysis was performed using Prism5 software (GraphPad). Data were analysed between multiple groups by one-way analysis ANNOVA followed by Bonferroni's post-hoc test p-value of <0.05 was considered statistically significant.

## 3. RESULTS

### 3.1 Beneficial Effects of H-DHPM on Survival

In MCT group, animals injected with MCT (60 mg/kg), 4 out of 15 animals died by 21 days of MCT exposure. Animals in MCT+ED group (H-DHPM treatment from day 0 of MCT injection), showed no mortality whereas one animal died in

MCT+LD group (H-DHPM treatment from day 14 of MCT injection) by 21 days. Furthermore animals in drug alone (H-DHPM) or in DMSO group all the animals survived. The survival index in relation to dosage is plotted by Kaplan-Meier method using GraphPad Prism5 in Fig. 1.

Additionally, we also observed a decrease in weight of rats that were given MCT as compared to control whereas H-DHPM treated rats showed no significant change in body weight as compared to control as shown in Table 2. Similarly, rats injected with DMSO also showed no significant change in body weight.

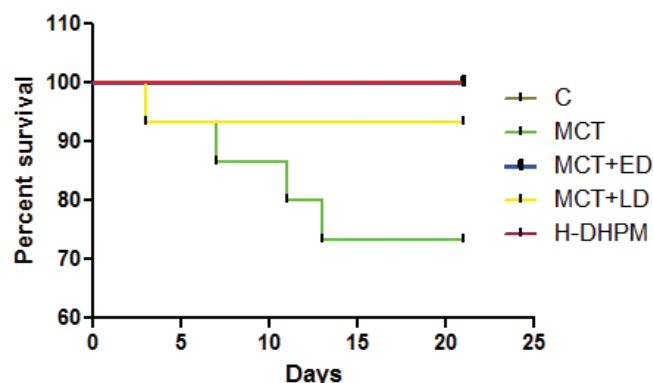


**Figure 1.** Effect of H-DHPM on MCT injected rats H-DHPM administered intraperitoneally (i.p.) at 30 mg/kg to MCT exposed rats at day 0 or day 14 significantly improved survival of rats as compared to MCT. After 21 days, 100 per cent survivorship was observed in C, MCT+ED, H-DHPM and DMSO where as 73.3 per cent survivorship was observed in MCT rats, 93.3 per cent survivorship was observed in H-DHPM+LD. n=15/group. Survival graph was plotted using Kaplan-Meier method and compared by Mantel-Cox Test. Using Prism5 (GraphPad). MCT vs C  $p<0.05$ .

### 3.2 H-DHPM Significantly Improves Pulmonary Hemodynamics

The RVSP in control group (c; n=15) which did not receive any drug was ( $22.6 \pm 1.8$  mmHg). There was a significant increase in RVSP in animals of group (n=11) that received MCT ( $46.2 \pm 0.88$  mmHg,  $p<0.05$ ). Furthermore, rats treated with H-DHPM from day zero of MCT treatment, MCT+ED group (n=15), showed significant decrease in RVSP as compared to MCT ( $23.2 \pm 1.45$  mmHg). Similarly, rats treated with H-DHPM from day 14 of MCT injection, MCT+LD (n=14) also showed a significant decrease in RVSP as compared to MCT ( $25.3 \pm 0.80$  mmHg). Additionally, in H-DHPM group (n=15) which received H-DHPM drug alone ( $22.3 \pm 1.2$  mmHg) did show any significant changes in RVSP as compared to control. Likewise, animals treated with DMSO only, DMSO group (n=15), showed no significant change in RVSP ( $21.9 \pm 0.8$  mmHg) (Fig. 2(a)). MCT injection or H-DHPM or vehicle treatment had no effect on systemic blood pressure in all animals (data not shown).

RVH, a hallmark of PH, was assessed by in all animals. FI in rats of control group (C) was  $0.36 \pm 0.03$  FI in MCT group rats was significantly increased ( $0.53 \pm 0.09$ ,  $p<0.05$ )

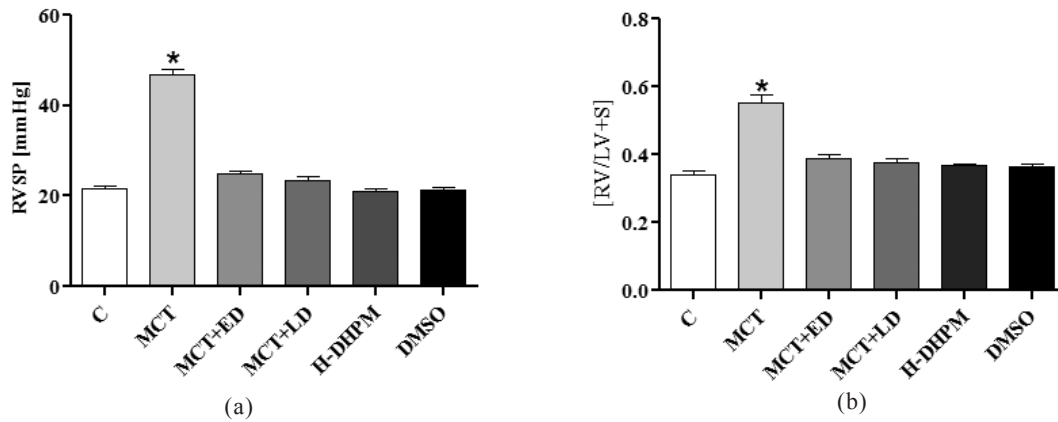


**Figure 2.** H-DHPM improves pulmonary hemodynamics in MCT injected animals (a) Graphical representation of RVSP plotted and analysed by Prim5 (GraphPad), which showed a significant increase in RVSP of animals insulted with MCT ( $46.2 \pm 0.88$  mmHg,  $*p < 0.05$  vs C) as compared to C ( $22.6 \pm 1.8$  mmHg). RVSP in H-DHPM+ED ( $25.3 \pm 0.80$  mmHg) and H-DHPM+LD ( $22.3 \pm 1.2$  mmHg), H-DHPM ( $22.3 \pm 1.2$  mmHg), DMSO ( $21.9 \pm 0.8$  mmHg) was non-significant as compared to C and (b) RVH was measured as wet weight of RV and LV+S by formula, RVH was highly significantly increased in MCT ( $0.53 \pm 0.09$  mmHg;  $*p < 0.05$  vs C) as compared to C ( $0.36 \pm 0.03$ ); whereas, non-significant H-DHPM+ED ( $0.39 \pm 0.05$  mmHg), H-DHPM+LD ( $0.38 \pm 0.02$  mmHg), H-DHPM ( $0.37 \pm 0.06$  mmHg) and DMSO ( $0.39 \pm 0.08$  mmHg) as compared to control.  $n = 15$ /group in C/H-DHPM/MCT+ED/DMSO;  $n = 11$  in MCT;  $n = 14$  in MCT+LD.

as compared to control group (Fig. 2(b)). Moreover, in H-DHPM+ED group rats FI ( $0.39 \pm 0.05$ ) was significantly alleviated as compared to MCT group (Fig. 2(b)). Similarly, rats in H-DHPM+LD, FI ( $0.38 \pm 0.02$ ) was significantly decreased as compared to MCT group. Animals in H-DHPM alone group ( $0.37 \pm 0.06$ ) and DMSO group ( $0.39 \pm 0.08$ ) showed no significant change in FI as compared to control. These findings clearly suggested that 30 mg/kg dose of H-DHPM attenuated pulmonary hypertension and right heart remodelling induced by MCT. All values were plotted and statistically analysed using Prim5 (GraphPad).

### 3.3 H-DHPM prevents Pulmonary Arterial Medial Wall Thickness

Another hallmark of progression of PH is the progressive increase in PVR, caused by the gradual increase in distal PA remodelling; which is assessed by calculating change in the arterial wall thickness by following % medial wall thickness (pMWT) =  $[(2 \times \text{medial thickness}) / \text{external diameter}] \times 100$ . Pulmonary arteries falling between diameters of 25  $\mu\text{m}$  - 200  $\mu\text{m}$  were analysed to quantify the medial wall thickness. We observed a significant increase in pMWT of MCT group rats ( $51.5 \pm 8.12\%$ ,  $p < 0.05$ ) as compared to the control group rats ( $25.5 \pm 10.12\%$ ) as shown in Fig. 3(a). Animals in H-DHPM+ED group had significant decrease in ( $27.9 \pm 10.10\%$ ) as compared to MCT group as shown in Fig. 3(a). Similarly, rats in H-DHPM+LD group

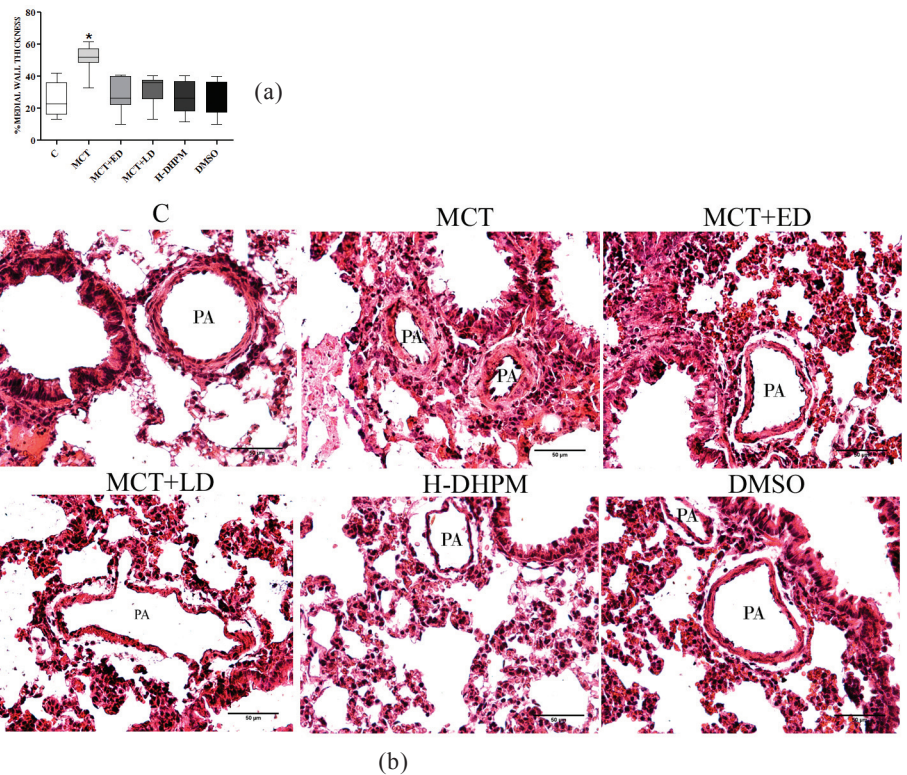


**Figure 3.** Preventive effect of H-DHPM on MCT induced pulmonary vascular remodelling (a) Arteries falling between 25 to 200  $\mu\text{m}$  of diameter were analysed using ImageJ and statistically analysed and plotted in Prim5 (GraphPad). Percent medial wall thickness in MCT ( $51.5 \pm 8.12\%$ ;  $*p < 0.05$  vs C) group was significantly increased as compared to C ( $25.5 \pm 10.12\%$ ). However, percent medial wall thickness in H-DHPM+ED ( $27.9 \pm 10.10\%$ ), H-DHPM+LD ( $33.7 \pm 7.10\%$ ), H-DHPM ( $26.4 \pm 10.1\%$ ) and DMSO ( $25.7 \pm 10.11\%$ ) were non-significant as compared to C. % medial wall thickness =  $[(2 \times \text{medial thickness}) / \text{external diameter}] \times 100$  in Prim5 (GraphPad) and (b) Representative H&E stained lung section images of different groups showing pulmonary artery remodelling. Images were captured by Olympus BX51 at 40x. Scale bar is 50  $\mu\text{m}$ ,  $n = 7$ /group.

also showed a significant decrease in pMWT ( $33.7 \pm 7.10$ ) as compared to MCT group. Rats in H-DHPM ( $26.4 \pm 10.1$ ) and DMSO ( $25.7 \pm 10.11\%$ ) group showed no change in pMWT. Representative images of pulmonary arteries of all animal groups are shown in Fig 3(b). These observations suggest H-DHPM significantly prevented remodelling of dPA induced by MCT. For analysis, 40 images were captured at 40x using Olympus Bx51 microscope (Olympus) and analysed/measured by ImageJ (NIH). The measured values statistically analysed were plotted using Prism5 GaphPad (Fig. 3(b)).  $n=7/\text{group}$ .

### 3.4 Early or Late Treatment with H-DHPM Prevented Pulmonary Parenchymal Tissue Remodeling in MCT-induced PAH Animal Model

Lung has the major population of pulmonary parenchymal cells which form the milieu of all pulmonary vessels. Hence,

it's of paramount importance to assess the morphological changes in pulmonary parenchyma in the course of disease. To access the effect of MCT and H-DHPM on pulmonary parenchymal remodelling, tissue sections were either stained with haematoxylin-eosin or Masson's trichrome stain. The former was used to assess the morphology of pulmonary parenchymal architecture, and later was used to assess the deposition of collagen in all groups. We observed, 21 days after MCT injection, the animals had developed a prominent structural remodelling in pulmonary parenchymal architecture which was attenuated by H-DHPM treatment in both groups H-DHPM+ED and H-DHPM+LD (Fig. 4(a)). Additionally we observed no prominent changes in pulmonary parenchymal architecture in H-DHPM or DMSO groups as compared to control (Fig. 4(a)). Moreover, we also observed increased intravascular infiltration, increased alveolar oedema and

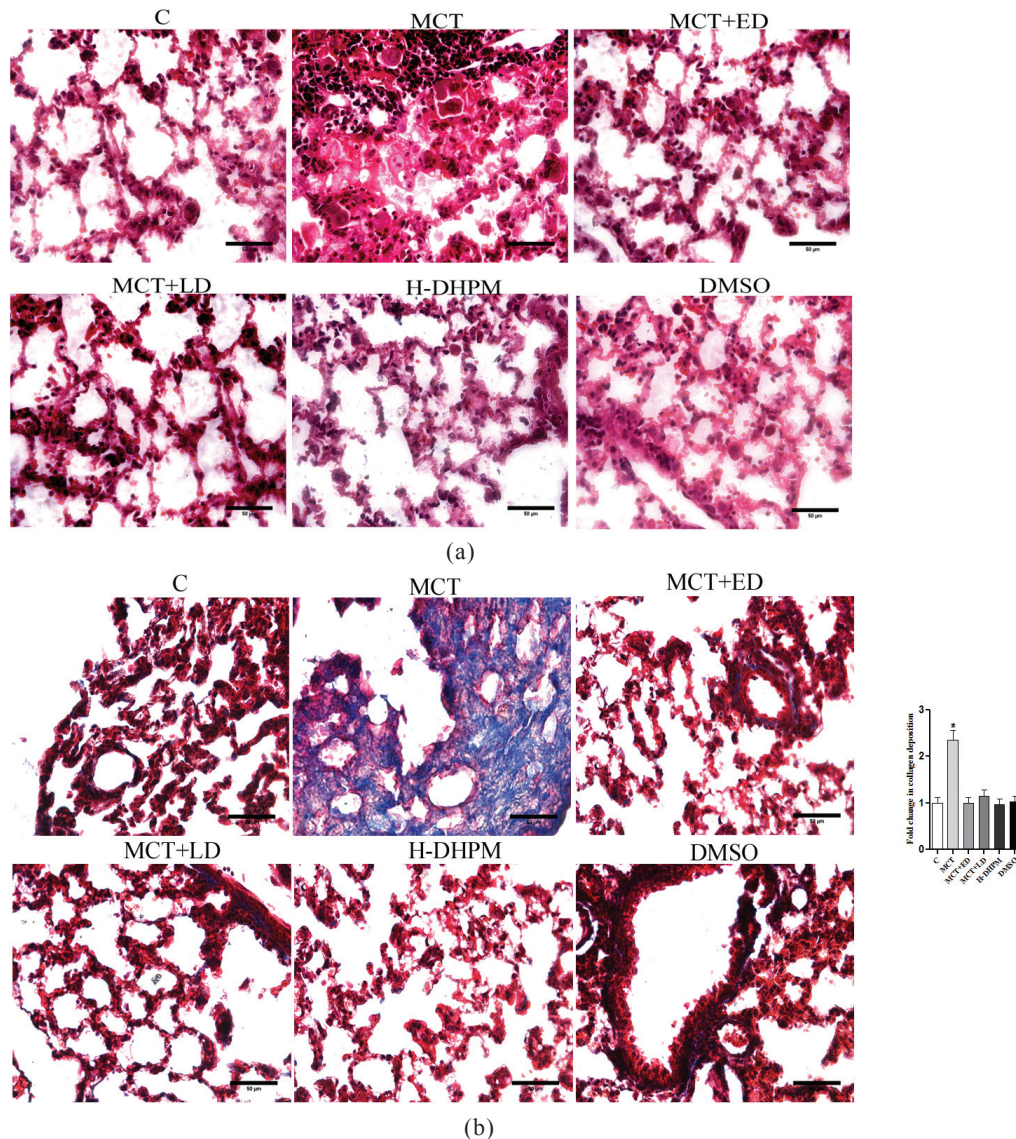


**Figure 4.** Pulmonary parenchymal remodelling regresses by treatment of H-DHPM in MCT injected rats (a) Representative images of H&E stained lung tissues showing prominent remodelling of alveolar architecture in MCT group. (b) Representation of Masson's Trichrome stained lung sections of rats. A marked increase of collagen deposition (blue colour) was observed in lung sections of MCT group, whereas no such observations were found in lung sections of H-DHPM treatment or DMSO groups. Images were taken at 40x by Olympus BX51 and analysed by ImageJ software. Scale bar is 50  $\mu\text{m}$ . Graphical representation of MTS stained sections showed 1.5 fold increase of collagen deposition in MCT lung sections only. Pixel intensity of blue color was calculated by ImageJ and plotted using Prism5 (GraphPad),  $n=7/\text{group}$ .

alveolar septal hyperplasia in rats insulted with MCT which was markedly mitigated by H-DHPM treatment. Furthermore, the MTS images showed a prominent collagen deposition (marked by blue colour) in lung tissues of MCT group animals as compared to control. On the contrary, animals in H-DHPM+ED and H-DHPM+LD groups had showed marked mitigated collagen deposition in lung tissues as compared to MCT group (Fig. 4(b)). The statistical evaluation of total collagen deposition was performed using ImageJ (NIH) and Prism5 (Graphpad) which is shown in Fig 4(b), and collagen deposition is represented as fold change as compared to control. As shown in graph, MCT group animals showed significant increase in collagen deposition (1.5 fold,  $p < 0.05$ ) as compared to control, whereas no such significant changes were observed in H-DHPM+ED, H-DHPM+LD, H-DHPM and DMSO group as compared to control. ( $n=7$ /group)

### 3.5 H-DHPM Induces Apoptosis to Prevent Remodeling of Pulmonary Arteries and Parenchyma

Considering the effect of intracellular calcium concentration on vascular remodelling, we assayed pulmonary tissues for apoptosis by TUNEL assay represented in Fig. 5(a). We observed a very minimum number of cells underwent apoptosis in MCT ( $4.17 \pm 0.64$ ) injected animals non-significant to control animals ( $2.3 \pm 0.51$ ). However MCT animals treated with H-DHPM showed very marked increase in TUNEL positive cells in both H-DHPM+ED ( $41.56 \pm 5.03$ ,  $p < 0.05$ ) and H-DHPM+LD ( $37.43 \pm 7.09$ ,  $p < 0.05$ ). Treatment of control rats with either H-DHPM ( $3.7 \pm 1.65$ ) or vehicle ( $3.53 \pm 1.85$ ) showed no increase or decrease in TUNEL positive cells as compared to control rats. Dnase I treated tissue sections used as a positive control (PC) showed highest percentage of TUNEL positive cells ( $59.36 \pm 4.50$ ,  $p < 0.05$ ). Representative images have been presented in Fig. 5(a) and graphically plotted in Fig. 5(b). TUNEL positive cells were counted by ImageJ, single blinded and obtained values were plotted in Prism5 (GraphPad) ( $n=7$ /group).

## 4. DISCUSSION

Our study for the first time showed use of novel DHP namely H-DHPM in MCT-induced PAH model. We clearly showed here that H-DHPM treatment in MCT injected rats significantly improved survival and prevented MCT induced PAH development and progression. Furthermore, our results affirm, H-DHPM precluded progression of pulmonary vascular and parenchymal remodelling and prevented right heart hypertrophy in H-DHPM treated rats as compared to MCT insulted rats. This is the first study of its kind that has shown cardio-pulmonary protective effect of H-DHPM in MCT induced PAH pathogenesis by RVSP, RVH, pulmonary vascular medial thickness and pulmonary tissue remodelling assessment.

MCT injected animal have been extensively used to study pathogenesis and therapeutic interventions of PAH<sup>6,7</sup>. The MCT animal model of PAH has been reported to be characterised by increased pulmonary artery medial wall thickness, vasculitis, and RV hypertrophy which ultimately might lead to increased mortality<sup>6,7</sup>. Corroborating previous literature we also observed after 3 weeks of MCT injection rats developed significant increase in RVSP, medial wall thickness of pulmonary arteries (25-200  $\mu\text{m}$ ) and RV hypertrophy. Although some studies have shown, MCT induces PAH by damaging the pulmonary endothelial cells (P-EC)<sup>20</sup>, however the exact toxicological mechanisms of MCT remains elusive. P-EC treated with MCT have been shown to develop either intracellular membrane disruptions or megalocytosis (characterised by an enlarged

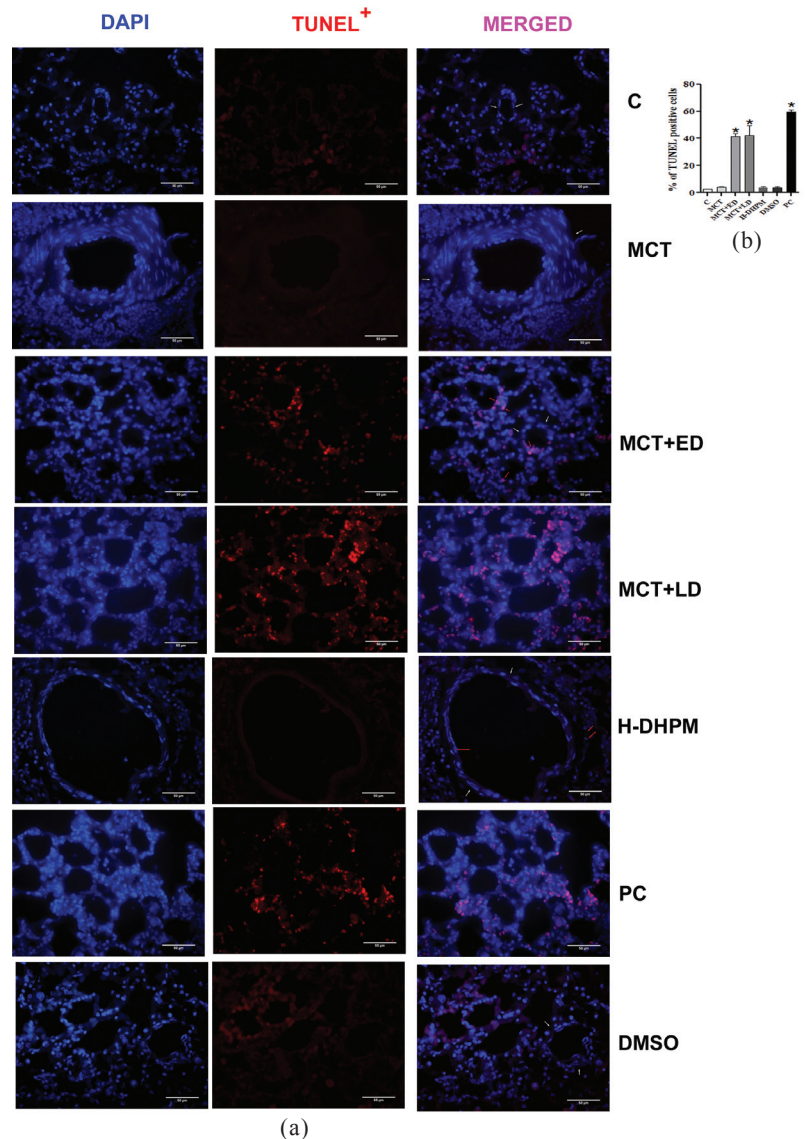


**Figure 5. H-DHPM induces apoptosis in lung parenchyma and lung vasculature (a) Representative images of TUNEL assay. (b) Assessment of TUNEL+ cells using ImageJ and Prism5 (GraphPad) showed no significant difference in percentage of TUNEL+ cells between C ( $2.3 \pm 0.51\%$ ), MCT ( $4.17 \pm 0.64\%$ ), H-DHPM ( $3.7 \pm 1.65$ ) and DMSO ( $3.53 \pm 1.85$ ) group lung sections. H-DHPM+ED ( $41.56 \pm 5.03$ ), H-DHPM+LD ( $37.43 \pm 7.09$ ) and DnaseI used as positive control ( $59.36 \pm 4.50$ ) showed significant ( $*p < 0.05$  vs C) increase in TUNEL+ cells as compared to C. Scale bar is 50 $\mu\text{m}$ ,  $n=7$ /group.**

Golgi apparatus)<sup>6,21</sup>. It has also been shown that MCT induced injury to vascular endothelium and myocardium results in an increase in Endothelin-1 (ET-1) release, a ligand of endothelin receptor A (ET<sub>A</sub>), subsequently leading to pathogenesis of PAH.<sup>21-23</sup> The ET<sub>A</sub> receptor is coupled to voltage-dependent Ca<sup>2+</sup> channels by G-proteins and shown to block Ca<sup>2+</sup> channels and eventually preventing ET<sub>A</sub> activation<sup>22,24</sup>. Calcium channel antagonism relieves injury of the pulmonary endothelium and the myocardium and rebalancing an interruption of the reactive oxidative species<sup>22,24</sup>. On the other hand, activation of the L-type Ca<sup>2+</sup> channels as a consequence of excess ET-1 expression results in pulmonary vasculature and the right ventricle remodelling<sup>20-24</sup>. On the contrary, in hypertrophic hearts, exogenous ET-1 neither modified right ventricular contractility nor systolic or diastolic Ca<sup>2+</sup> handling<sup>20-24</sup>. Intracellular Ca<sup>2+</sup> also acts a secondary messenger and its imbalance can induce pulmonary arterial smooth muscle cell (PASMC) proliferation<sup>25,26</sup>. Consequently, it can be interpreted that Ca<sup>2+</sup> channels play important role in pathogenesis of MCT induced PAH. Recently, H-DHPM has been discovered as a versatile L-type CCB capable of antiplatelet and antithrombotic activity, owing to single acyl (heptanoyl) group at the C4' position of DHPM molecule<sup>17,18</sup>. In the current study we used 30mg/kg dose of H-DHPM to evaluate its effect on PAH pathogenesis. A general consensus on the course of PAH pathogenesis dictates the pathogenesis of PAH a two phase malady<sup>27</sup>. First phase involves the injury and 2<sup>nd</sup> phase involves the progression. To evaluate if H-DHPM can prevent the early onset and the progression of pathogenesis in PAH, we used two study protocols, in one group we dosed rats with H-DHPM from day zero of MCT injection and in other group we dosed rats with H-DHPM from day 14 of MCT injection. In both treatment groups we observed significant decrease in RVSP and medial wall thickness in comparison to MCT injected animals. These observations clearly demonstrated that H-DHPM is protective, i.e. it protects the vascular walls from early toxic effects of MCT. Of note, H-DHPM when given after 14 days of MCT injection not only prevented the progression but reversed the effects of MCT as no change was observed in RVSP and medial wall thickness of pulmonary arteries (25 µm - 200 µm) in these animals. MCT leads to right heart remodelling by directly injuring the myocardium and additionally by increasing pulmonary vascular resistance through angio-obliterative proliferation of medial wall, which has been previously proven to be somewhat prevented by different CCBs. Substantiating these studies we also observed a decrease in RVH of animals treated with H-DHPM as compared to MCT insulted rats.

Previous studies have shown rats with MCT-induced pulmonary hypertension also exhibits a prominent decrease in lung compliance, which can be attributed to pulmonary parenchymal transdifferentiation, alveolar oedema and alveolar septal cell hyperplasia<sup>6,28</sup>. Since the lung dysfunction could exacerbate MCT induced progression of pulmonary vascular remodelling, it is essential to evaluate the effect of H-DHPM on pulmonary parenchymal tissue in MCT-treated rats. We observed a prominent loss of pulmonary parenchymal architecture in MCT rats which was markedly prevented by H-DHPM treatment in both treatment groups. Additionally, we

also observed decreased intravascular infiltration, decreased alveolar oedema and alveolar septal hyperplasia in rats treated with H-DHPM. Moreover, histopathological study has revealed MCT-treated animals have marked interstitial hypercellularity and fibrosis<sup>6</sup>. Pulmonary tissues of MCT injected rats have excessive collagen secretion and fibrosis.<sup>6</sup> Significant increase in collagen deposition was observed in our study after 3 weeks of MCT exposure. The collagen deposition was prominent in remodelled pulmonary parenchyma and vasculature. However, early or late treatment both prevented the collagen deposition in rat lungs.

Clinical or experimental studies on PAH have attributed the pulmonary vascular pathology to change in cell phenotype, pro-angiogenic niche formation and apoptosis resistant vascular cells<sup>29</sup>. Further it's been shown that these vascular cells especially PASMC and P-EC exhibit quasi-cancerous features that induce over proliferative demand in these tissues<sup>30</sup>. On the contrary, some studies have reported MCT administration results in endothelial injury which triggers the transformation of PASMC into more proliferative and apoptosis resistant phenotype which could be an explanation of hyperplasia of PASMC and lack of plexiform lesions in MCT induced PAH animal model<sup>31,32</sup>. Here we reported, pulmonary sections assessed for apoptotic cells by TUNEL assay showed very little apoptotic cells in MCT injected animals which was non-significant to the control animals. However, H-DHPM treatment in MCT insulted animals significantly increased number of apoptotic cells as compared to in MCT alone insulted animals. Interestingly, these TUNEL positive cells were only observed in H-DHPM treated MCT animals whereas no apoptotic cells were observed in drug alone group. Hence these findings clearly suggest that H-DHPM induced apoptosis in diseased proliferative cells only that subsequently vetoed vascular muscularisation or intimal remodelling, subsequently decreased PVR. In addition, we observed H-DHMP induced apoptosis in diseased pulmonary tissue and consequently declines fibrinoproliferative axis hence prevents the development of fibrosis or pulmonary alveolar destruction whereas in drug alone groups no such apoptotic cells were observed.

NO is a well-known vasodilator and has been used as a therapy to treat PAH. It has been speculated that the early endothelial damage in MCT animal models is responsible for a low level of NO in the pulmonary vessels<sup>1,2,6</sup>. However, a persistent NO is biosynthesised and a sustained release is maintained for normal vascular vasodilatation response<sup>1,2,6</sup>. However, under persistent toxic insult of MCT at later stages the bioavailability of NO is compromised significantly, subsequently resulting in impaired vascular patency. NO interacts with Guanylate cyclase via its heme group and plays regulatory role in conversion of GTP to cGMP. cGMP triggers a reduction in [Ca<sup>2+</sup>]<sub>i</sub> concentration through the activation of cGMP-dependent protein kinase (PKG)<sup>33</sup>. This mechanism influences smooth muscle cell proliferation, hypertrophy, contraction and platelet aggregation related PAH pathogenesis<sup>33</sup>. H-DHPM, arrests biphasic calcium entry, thereby eliminating calcium cross talk and suggesting the direct stimulatory action of Ca<sup>2+</sup>-channel blockers on endothelial NO production<sup>17,18</sup>. Further, these studies have proven that

H-DHPM improves balance between eNOS/iNOS in both preclinical and translational studies. Besides, these studies proved the efficacy of H-DHPM was better than amlodipine in terms of NO production. Inhibiting platelet aggregation and cCGMP; henceforth, projecting H-DHPM as a possible.

The main focus of our study was to identify the beneficial effects of novel DHP molecule H-DHPM in MCT-induced PAH model. In conclusion, irrespective of the mechanism or mechanisms involved, H-DHPM inhibits pulmonary artery hypertension and right ventricular hypertrophy in MCT-treated rats, as well as minimizes the severity of MCT-induced morphologic changes in the pulmonary vasculature and parenchyma. Notably, H-DHPM not only prevented the early onset toxic effects of MCT but also reversed the onset and prevented the progression of PAH pathogenesis.

## 5. LIMITATIONS OF THE STUDY

This study was intended to assess the role of the H-DHPM, a novel DHP compound in preventing the development of MCT induced pulmonary hypertension in rats. The major limitation of study was not assessing any mechanistic study to associate the preventive impact of drug on any particular pathway. Since the drug is pleiotropic; its precise mechanism of action in prevention of pulmonary hypertension needs to be further evaluated in future studies.

## CONFLICT OF INTEREST

None of the authors any conflict of interest to declare.

## REFERENCES

1. Stenmark, K.R.; Meyrick, B.; Galie, N.; Mooi, W.J.; & McMurtry, I.F. Animal models of pulmonary arterial hypertension: the hope for etiological discovery and pharmacological cure. *Am. J. Physiol. Lung Cell Mol. Physiol.*, 2009, **297**: L1013–L1032. doi:10.1152/ajplung.00217.2009.
2. Umar, S.; Steendijk, P.; Ypey, D.L.; Atsma, D.E.; van der Wall, E.E.; S chali, M.J. & van der Laarse, A. Novel approaches to treat experimental pulmonary arterial hypertension: A review. *J. Biomed. Biotechnol.*, 2010, pp.11. doi:10.1155/2010/702836.
3. Farber, H.W. & Loscalzo, J. Pulmonary arterial hypertension. *N. Engl. J. Med.*, 2004, **351**, 1655–1665. doi: 10.1056/NEJMra035488
4. Voelkel, N.F. & Cool, C. Pathology of pulmonary hypertension. *CardiolClin.*, 2004, **22**, 343–351. doi: 10.1016/j.ccl.2004.04.010
5. Rubin, L.J.; Simonneau, G.; Badesch, D.; Galiè, N.; Humbert, M.; Keogh, A.; Massaro, J; Matucci Cerinic, M.; Sitbon, O. & Kymes, S. The study of risk in pulmonary arterial hypertension. *Eur. Respir. Rev.*, 2012, **21**, 234–238. doi: 10.1183/09059180.00003712.
6. Gomez-Arroyo, J.G.; Farkas, L.; Alhussaini, A.A.; Farkas, D; Kraskauskas, D.; Voelkel, N.F. & Bogaard, H.J. The monocrotaline model of pulmonary hypertension in perspective. *Am J Physiol Lung Cell Mol Physiol.*, 2012, **302**, L363–L369. doi: 10.1152/ajplung.00212.2011.
7. Xiao, R.; Su, Y.; Feng, T.; Sun, M.; Liu, B.; Zhang, J.; Lu, Y.; Li, J.; Wang, T.; Zhu, L. & Hu, Q. Monocrotaline induces endothelial injury and pulmonary hypertension by targeting the extracellular calcium-sensing receptor. *J. Am. Heart Assoc.* 2017, **6**, e004865. doi:10.1161/JAHA.116.004865.
8. Rodman, D.M.; Harral, J.; Wu, S.; West, J.; Hoedt-Miller, M.; Reese, K.A. & Fagan, K. The low-voltage-activated calcium channel CAV3.1 controls proliferation of human pulmonary artery myocytes. *Chest*, 2005, **128**, 581S–582S. doi: 10.1378/chest.128.6\_suppl.581S.
9. Rodman, D.M.; Reese, K.; Harral, J.; Fouty, B.; Wu, S.; West, J.; Hoedt-Miller, M.; Tada, Y.; Li, K.X.; Cool, C.; Fagan, K. & Cribbs, L. Low-voltage-activated (T-type) calcium channels control proliferation of human pulmonary artery myocytes. *Circ Res.*, 2005, **96**, 864–872. doi: 10.1161/01.RES.0000163066.07472.ff.
10. Paffett, M.L.; Riddle, M.A.; Kanagy, N.L.; Resta, T.C. & Walker, B.R. Altered protein kinase C regulation of pulmonary endothelial store- and receptor-operated Ca<sup>2+</sup> entry after chronic hypoxia. *J Pharmacol Exp Ther.*, 2010, **334**, 753–760. doi: 10.1124/jpet.110.165563.
11. Robertson, T.P.; Hague, D.; Aaronson, P.I. & Ward, J.P. Voltage independent calcium entry in hypoxic pulmonary vasoconstriction of intrapulmonary arteries of the rat. *J. Physiol.*, 2000, **525**, 669–680. doi: 10.1111/j.1469-7793.2000.t01-1-00669.x
12. Sajkov, D.; Wang, T.; Frith, P.A.; Bune, A.J.; Alpers, J.A. & McEvoy, R.D. A comparison of two long acting vasoselective calcium antagonists in pulmonary hypertension secondary to COPD. *Chest*, 1997, **111**, 1622–1630. doi: 10.1378/chest.111.6.1622
13. Kleinbloesem, C.H.; van Brummelen, P.; Danhof, M.; Faber, H.; Urquhart, J. & Breimer, D.D. Rate of increase in the plasma concentration of nifedipine as a major determinant of its hemodynamic effects in humans. *Clin. Pharmacol. Ther.*, 1987, **41**:26–30. doi: 10.1038/clpt.1987.5
14. Rubin, L.J. & Moser, K. Long-term effects of nitrendipine on hemodynamics and oxygen transport in patients with cor pulmonale. *Chest*, 1986, **89**, 141–145. doi: 10.1378/chest.89.1.141
15. Saadjian, A.Y., Philip-Joet, F. & Arnaud, A. Hemodynamic and oxygen delivery: responses to nifedipine in pulmonary hypertension secondary to chronic obstructive lung diseases. *Cardiology*, 1987, **74**, 196–204. doi: 10.1159/000174197
16. Manral, S.; Bhatia, S.; Sinha, R.; Kumar, A.; Rohil, V.; Arya, A; Dhawan, A.; Arya, P.; Joshi, R; Sreedhara, S.C.; Gangopadhyay, S.; Bansal, S.K.; Chatterjee, S.; Chaudhury, N.K.; V ijayan, V.K.; Saso, L.; Parmar, V.S.; DePass, A.L.; Prasad, A.K. & Raj, H.G. Normalisation of deranged signal transduction in lymphocytes of COPD patients by the novel calcium channel blocker H-DHPM.

- Biochimie*, 2011, **93**, 1146-1156.  
doi: 10.1016/j.biochi.2011.04.004.
17. Bhatewara, A.; Jetti, S.R.; Kadre, T.; Paliwal, P.; & Shubha, J. Microwave-Assisted synthesis and biological evaluation of dihydropyrimidinone derivatives as anti-inflammatory, antibacterial, and antifungal agents. *Int J Med Chem.*, 2013, Article ID **197612**, 5 pages.  
doi: 10.1155/2013/197612.
  18. Priya, N.; Singh, P.; Bhatia, S.; Medhi, B.; Prasad, A.K.; Parmar, V.S. & Raj, H.G. Characterisation of a unique dihydropyrimidinone, ethyl 4-(4-heptanoyloxyphenyl)-6-methyl-3,4-dihydropyrimidin-2-one-5-carboxylate, as an effective antithrombotic agent in a rat experimental model. *JPP*, 2011, **63**, 1175–1185.  
doi: 10.1111/j.2042-7158.2011.01316.x.
  19. Gorenflo, M.; Vogel, M.; Hetzer, R.; Schmitz, L.; Bein, G.; Alexi, V. & Lange, P.E. Morphometric techniques in the evaluation of pulmonary vascular changes due to congenital heart disease. *Path. Res. Pract.*, 1996, **192**, 107–116.  
doi: 10.1016/S0344-0338(96)80204-4
  20. Nogueira-Ferreira, R.; Vitorino, R.; Ferreira, R. & Henriques-Coelho, T. Exploring the monocrotaline animal model for the study of pulmonary arterial hypertension: a network approach. *Pulm. Pharmacol. Ther.*, 2015, **35**, 8-16.  
doi: 10.1016/j.pupt.2015.09.007.
  21. Zhang, T.T.; Cui, B.; Dai, D.Z. & Su, W. CPU 86017, p-chlorobenzyltetrahydroberberine chloride, attenuates monocrotaline-induced pulmonary hypertension by suppressing endothelin pathway. *Acta Pharmacol. Sin.*, 2005, **26**, 1309–1316.  
doi: 10.1111/j.1745-7254.2005.00214.x.
  22. Wolkart, G.; Stromer, H.; & Brunner, F. Calcium handling and role of endothelin-1 in monocrotaline right ventricular hypertrophy of the rat. *J Mol Cell Cardiol*; **32**, 1995–2005.
  23. Mawatari, E.; Hongo, M.; Sakai, A.; Terasawa, F.; Takahashi, M.; Yazaki, Y.; Kinoshita, O. & Ikeda, U. Amlodipine prevents monocrotaline-induced pulmonary arterial hypertension and prolongs survival in rats independent of blood pressure lowering. *CEPP*. 2007, **34**, 594–600.  
doi: 10.1111/j.1440-1681.2007.04618.x.
  24. Brunner, F.; Wolkart, G. & Haleen, S. Defective intracellular calcium handling in monocrotaline-induced right ventricular hypertrophy: protective effect of long-term endothelin-A receptor blockade with 2-Benzo[1,3]dioxol-5-yl-3-benzyl-4-(4-methoxy-phenyl)-4-oxobut-2-enoate-sodium (PD 155080). *JPET*, 2002, **300**, 442–449.  
doi: 10.1124/jpet.300.2.442
  25. Humbert, M.; Morrell, N.W.; Archer, S.L.; Stenmark, K.R.; MacLean, M.R.; Lang, I.M.; Christman, B.W.; Weir, E.K.; Eickelberg, O.; Voelkel, N.F. & Rabinovitch, M. Cellular and molecular pathobiology of pulmonary arterial hypertension. *J. Am. Coll. Cardiol.*, 2004, **43**, S13-S24.  
doi: 10.1016/j.jacc.2004.02.029
  26. Morrell, N.; Adnot, S.; Archer, S.; Dupuis, J.; Jones, P.; MacLean, M.R.; McMurtry, I.F.; Stenmark, K.R.; Thistlethwaite, P.A.; Weissmann, N.; Yuan, J.X. & Weir, E.K. Cellular and molecular basis of pulmonary arterial hypertension. *J. Am. Coll. Cardiol.* 2009, **54**, S20-S31.  
doi: 10.1016/j.jacc.2009.04.018.
  27. Chester, A.H. & Yacoub, M.H. The role of endothelin-1 in pulmonary arterial hypertension. *Glob. Cardiol. Sci. Pract.* 2014, **2**, 62–78.  
doi: 10.5339/gcsp.2014.29
  28. Dumitrascu, R.; Koebrich, S.; Dony, E.; Weissmann, N.; Savai, R.; Pullamsetti, S.S.; Ghofrani, H.A.; Samidurai, A.; Traupe, H.; Seeger, W.; Grimminger, F. & Schermuly, R.T. Characterisation of a murine model of monocrotaline pyrrole-induced acute lung injury. *BMC Pulm Med.*, 2008, **8**(25), 15 p.  
doi: 10.1186/1471-2466-8-25.
  29. Voelkel, N.F.; Gomez-Arroyo, J.; Abbate, A.; Bogaard, H.J. & Nicolls, M.R. Pathobiology of pulmonary arterial hypertension and right ventricular failure. *Eur. Respir. J.*, 2012, **40**, 1555–1565.  
doi: 10.1183/09031936.00046612.
  30. Rai, P.R.; Cool, C.D.; King, J.A.C.; Stevens, T.; Burns, N.; Winn, R.A.; Kasper, M. & Voelkel, N.F. The Cancer Paradigm of Severe Pulmonary Arterial Hypertension. *Am. J. Respir. Crit. Care Med.*, 2008; **178**, 558–564.  
doi: 10.1164/rccm.200709-1369PP
  31. Nogueira-Ferreira, R.; Ferreira, R. & Henriques-Coelho, T. Cellular interplay in pulmonary arterial hypertension: implications for new therapies. *Biochim. Biophys. Acta.*, **1843**, 885–893.  
doi: 10.1016/j.bbamcr.2014.01.030.
  32. Malenfant, S.; Neyron, A.; Paulin, R.; Potus, F.; Meloche, J.; Provencher, S. & Sébastien, B. Signal transduction in the development of pulmonary arterial hypertension. *Pulm Circ.* 2014, **3**, 278–293.  
doi: 10.4103/2045-8932.114752.
  33. Carvajal, J.A.; Germain, A.M.; Huidobro-Toro, J.P.; & Weiner, C.P. Molecular mechanism of cGMP-mediated smooth muscle relaxation. *J Cell Physiol.* 2000, **184**, 409–42.  
doi: 10.1002/1097-4652(200009)184:3<409::AID-JCP16>3.0.CO;2-K

#### ACKNOWLEDGMENTS

The study was funded under project DRDO, Ministry of Defence, Govt. of India. SMM received fellowship from Council of Scientific and Industrial Research, India. Author received fellowship from University Grants Commission, India and also received fellowship from DRDO, India.

#### CONTRIBUTORS

**Mr Shajer M. Malik** has received his MSc in Toxicology (Life Science) from Jamia Hamdard University. Currently, he is working as a Senior Research Fellow at Department of Physiology, Defence Institute of Physiology and Allied Science,

Delhi. He is interested in the elucidating pathomechanisms of high altitude associated pulmonary hypertension and identifying the key therapeutic targets.

In the current study, he was involved in execution of experimental studies, data collection, data analysis and manuscript writing

**Dr Satyanarayan Deep** has received his PhD in Life Sciences from Bharathair University. He has various publications on his name. His area of research was to understand molecular cause of neurodegeneration at high altitude.

He was involved in execution of experiments and manuscript writing.

**Mr Rahul Ranjan** has done MSc in Biomedical Science from University of Delhi. Currently he is working as a senior research fellow at department of Neurobiology, Defence Institute of Physiology and Allied Sciences, Delhi. He is interested in studying hypobaric hypoxia induced neurodegeneration.

In the current study, he has involved in execution of experimental studies, data collection and manuscript writing

**Prof. A.K. Prasad** obtained his PhD from University of Delhi. His major research interest lies in the areas : Biocatalysis and biotransformations, polymeric architecture & supra-molecular chemistry and synthesis of modified nucleosides and bioactive heterocycles.

In the current study, H-DHPM was synthesised, characterised and provided by him.

**Dr Dipti N. Prasad** is Scientist 'F' and Head of Neurobiology Department, Defence Institute of Physiology and Allied Sciences, Delhi. She has supervised many graduated students and has publications in various national and international journals. She was involved in reviewing and drafting of the current manuscript.

**Dr Shashi B. Singh**, Director General, Life Sciences, DRDO. She has immensely contributed to the understanding of high altitude physiology and pioneered the development of nutraceuticals and prophylactics for several high altitude maladies that include hypophagia and cognitive impairment.

She was involved in reviewing and drafting of the current manuscript.

**Dr Ekta Kohli** is Scientist 'E' at Defence Institute of Physiology and Allied Sciences, Delhi. Her major research area is Nanotechnology and Toxicology. She has publications in various national and International journals, chapters, and patent to her credit.

She has contributed in thorough experimental design, execution, analysis, interpretation of results and writing of the manuscript.